# ATOMISTIC STUDY OF THE EFFECT OF MAGNESIUM DOPANTS ON NANOCRYSTALLINE ALUMINIUM

A Thesis

Submitted to the Faculty

of

Purdue University

by

Amirreza Kazemi

In Partial Fulfillment of the

Requirements for the Degree

of

Master of Science in Mechanical Engineering

August 2019

Purdue University

Indianapolis, Indiana

# THE PURDUE UNIVERSITY GRADUATE SCHOOL
# STATEMENT OF COMMITTEE APPROVAL

Dr. Shengfeng Yang

Department of Mechanical and Energy Engineering

Dr. Jing Zhang

Department of Mechanical and Energy Engineering

Dr. Likun Zhu

Department of Mechanical and Energy Engineering

**Approved by:**

Dr. Sohel Anwar

Chair of the Graduate Program

I dedicate this thesis to my parents who have been supporting me emotionally and financially support me and especially my sister, who is inspiring me to follow my dreams.

# ACKNOWLEDGMENTS

I would like to thank Dr. Shengfeng Yang for his exceptional learning and research opportunity, along with his endless academic and financial support during my master thesis and provisions above the academic contexts. I would like to thank my committee members for their assistance and supervision in the preparation of this thesis. Finally, I reserve a special thanks to my family for their support and encouragement.

TABLE OF CONTENTS

Page

# LIST OF FIGURES

Figure Page

# ABBREVIATIONS

| | |
|---|---|
| BCC | Body Center Cubic Structure |
| FCC | Face Center CubicS tructure |
| HCP | Hexagonal Close-Packed |
| MD | Molecular Dynamics |
| MC/MD | Monte Carlo/Molecular Dynamics |
| Mg | Magnesium |
| Al | Aluminum |
| NC | Nanocrystalline |
| GB | Grain Boundary |
| CNA | Common Neighbor Analysis |

# ABSTRACT

Kazemi, Amirreza. Purdue University, August 2019. Atomistic Study of the Effect of Magnesium Dopants on Nnanocrystalline Aluminium. Major Professor: Shengfeng Yang.

Atomistic simulations are used in this project to study the deformation mechanism of polycrystalline and bicrystal of pure Al and Al-Mg alloys. Voronoi Tessellation was used to create three-dimensional polycrystalline models. Monte Carlo and Molecular Dynamics simulations were used to achieve both mechanical and chemical equilibrium in all models. The first part of the results showed improved strength, which is included the yield strength and ultimate strength in the applied tensile loading through the addition of 5 at% Mg to nanocrystalline aluminum. By viewing atomic structures, it clearly shows the multiple strengthening mechanisms related to doping in Al-Mg alloys. The strength mechanism of dopants exhibits as dopant pinning grain boundary (GB) migration at the early deformation stage. At the late stage where it is close to the failure of nanocrystalline materials, Mg dopants can stop the initiation of intergranular cracks and also do not let propagation of existing cracks along the GBs. Therefore, the flow stress will improve in Al-Mg alloy compared to pure Al. In the second part of our results, in different bicrystal Al model, $\sum 3$ model has higher strength than other models. This result indicates that GB structure can affect the strength of the material. When the Mg dopants were added to the Al material, the strength of sigma 5 bicrystal models was improved in the applied shear loading.

However, it did not happen for $\sum 3$ model, which shows Mg dopants cannot affect the behavior of this GB significantly. Analysis of GB movements shows that Mg dopants stopped GBs from moving in the $\sum 5$ models. However, in sigma 3 GBs, displacement of grain boundary planes was not affected by Mg dopants. Therefore, the strength and flow stress are improved by Mg dopants in $\sum 5$ Al GBs, not in the $\sum 3$ GB.

# 1. INTRODUCTION

## 1.1 Background

Nanomaterials are widely using nowadays and have been a popular subject for research in the field of material science. When compared nanomaterials with coarse-grained materials, these nanomaterials have lots of excellent structural and functional properties which are caused to be useful in different applications. One of the popular nanomaterials which are used in most of the research is nanocrystalline aluminum because of its application in different areas, such as solar back plants, design of cars, and explosives.

Nanocrystalline materials have some physical, mechanical, and chemical properties that researchers are interested in using these materials. High strength, superior hardness, and high wear resistance are some of the properties which are implemented in different applications [1, 2].

Furthermore, besides high strength in materials, good ductility is another parameter which is required in nanomaterials to avoid catastrophic or failure in the tests. However, there are some metallic materials which have high strength besides low ductility [3, 4], which limits the utility of this material. Combination of these both properties makes them the best materials for structural and functional applications such as medicine, energy, and transportation. The mechanisms to produce high ductility material and analyze the approaches to get good ductility is important in nanocrystalline alloys.

Many strategies are available to increase the strength and elasticity in Nanocrystalline materials that are deliberated in experimental and theoretical analysis. Addition of dopants is one of the best ways for improving the strength and hardness of materials.

## 1.2 Objective

In this first part of this study, we focus on using atomistic simulations to find out the atomic-level mechanism of GB segregation strengthening of nanocrystalline Al by doping Mg atoms. The main objective of this study is the effect of Mg on the behavior of Al material in applied loading. We used three-dimensional polycrystalline models for both Al and Al-5% Mg, and tensile loading was conducted on both Al and Al-Mg alloys to explore the effect of Mg dopants on the mechanical properties of NC Al. All tensile tests were conducted through atomistic simulation.

In the second part of this study, we used bicrystal models instead of polycrystal models to explore the behavior of Mg dopants on the strength of NC Al. Models are created for both Al and Al-3.5%Mg alloys. Shear loading was used on both models to find out the effect of dopants on the strength of materials. The atomistic simulation was used for both alloys in the atomic-level mechanisms.

This research consists of six chapters, and it is organized as follows. In the first chapter, we introduce briefly about materials and properties that are used in different applications and explain what our goals in this study are. In chapter 2, we review literature about Al alloys, polycrystal, and bicrystal materials, and deformation mechanisms of materials.

We describe molecular dynamics methods, Voronoi tessellation, and common neighbor analysis, which are used in our models for creation and analysis parts in the third chapter of this study. Chapter four and five are the main parts of this study which show simulation details of our models in polycrystal and bicrystal models and present results of models after loadings and discusses what are observed in MD simulations. In the last part of this study, chapter 6, we explain the summary of our work and directions for future work.

# 2. LITERATURE REVIEW

## 2.1 Applications of Aluminum Alloys

Aluminum is one of the accessible materials which improve physical properties by alloying with different materials to generate unique properties such as resistance to failure or heat. More research needs for alloying elements, and it is not easy to process for doing experimental and simulations for getting acceptable results. For example, the effect of the addition of such elements can be explained here. Carbon can raise tensile stress, hardness, and resistance, but it can reduce ductility and toughness when adds to steel. Also, steel with chromium will increase strength, hardness, toughness, and scaling at high temperatures [5].

Aluminum is a material that we used more in our experiment. Aluminum is a lightweight metal that has excellent corrosion resistance, and anodizing can raise scratch resistance [6]. Aluminum is not like carbon steel in toughness because in low temperature can retain its toughness.

Aluminum is reflective, and that is why it is used in decorative applications or in contact with foodstuffs. Aluminum is a perfect conductor of heat and electricity. For example, comparing between copper and aluminum, conductivity in aluminum is almost twice copper in the same weigh. Ready for recycling and a wide variety of forming processes are excellent properties of this material.

## 2.2 Polycrystal Aluminum

Material properties such as high ultimate strength and superior hardness are important reasons widely usage of nanocrystalline (NC) materials in various applications, but we cannot ignore some behaviors which limited some applications of the

material [7,8]. The large volume fraction of high-energy interfacial regions, low thermal stability, and low ductility of NC materials are these properties which are caused useless in some cases. Pun et al. [2]. In experimental test added Mg during mechanical milling by low homologous temperature annealing treatments to add dopants without grain growth. They showed that hardness of Al-7% Mg is almost three times more than pure nanocrystalline Al and segregation caused the metal to become stronger and lightweight metal [2]. Unstable metal alloys are one of the problems in some materials that need to be solved. For example, Chookajorn worked enhancing the stability of Ti by adding W in the high temperature. Addition of dopants helps the low thermal stability of Ti to increase [3].

Embrittlement of materials can be controlled by interactions between grain boundaries. Segregation of dopants can change the behavior of grain boundaries. So by changing behaviors of GBs, ductility of materials will be changed [4]. Alloying NC materials with different elements is an effective way for improving thermal stability at high temperatures, can increase ductility, and further increase strength. These alloying elements will be distributed randomly in the grain interior as solid solutions or grain boundaries. When dopants added to grain boundaries chemistry of GBs changed, and as a result, it helped transformations in GB complexions [9–13] and therefore, affect the material properties [5,6,14–17].

In the first part, we work on Al-Mg alloys; researchers find out that Mg dopants can improve properties of materials through the solid solution strengthening [7, 8] and precipitates pinning GBs [18, 19] which includes improving yield strength and strain hardening. Lee [7] showed in his research small amount of Mg can affect significantly higher strength and ductility compared pure Al, and he concluded that both ductility and strength of Al-Mg alloys would improve by different amount of Mg by using experimental tests and also confirmed completely by molecular dynamic simulations how the high-strength alloys could exhibit high ductility. In addition, pun et al [2]. worked on the effect of Mg on nanocrystalline Al, and they identified that GB segregation strengthening could help improve the strength and hardness of

Al-Mg alloys. Based on studies, it showed that Mg atoms like to segregate to GBs, so GB segregation strengthening is more effective than solid solution strengthening in Al-Mg alloys, but there is no research on the behavior of the effect of Mg dopants that are segregated to GBs and improve the strength of NC Al in atomic level mechanisms. Moreover, [18] showed Mg dopants could stabilize the grain growth when it is added to NC Al at elevated temperature. They also showed coupled MC/MD simulation guided experimental for improving resistance to thermally induced grain coarsening in lightweight Al-Mg alloys and tried to extend the limited upper application of nanocrystalline alloy in high temperature which used thermodynamic and kinetic stabilization approach. However, it is still unknown the stabilization of the grain sizes of NC Al during the deformation process when Mg atoms are added to materials. Sauvage analyzed the segregation and precipitation mechanisms in Al-Mg alloys which in room temperature formed mostly nanoscaled and at 200 c more uniformed structure at severe plastic deformation (SPD) and concluded that segregation could contribute to the strengthening of these alloys.

## 2.3 Bicrystal Aluminum

By comparing conventional coarser-grained materials and nanostructured materials, we can understand that nanostructured material has superior mechanical properties, which are caused widely used in structural applications. These properties include high yield and fracture strength, superior wear resistance, high fatigue resistance, etc. these characters of nanostructured materials caused great interests for researchers to do research on mechanical properties and specifically deformation mechanisms. As mentioned, experimental work is difficult, and computer simulations are a powerful tool to gain more information in the fundamental knowledge based on atomistic models.

Interfaces between two different oriented crystals of the same materials can create grain boundaries. The structure and deformation characteristics of grain boundaries

can be studied in both experimental and computational methods, which is important by progress in tools in experimental like high-resolution transmission electron microscope and molecular dynamics in computational mechanics.

Many types of research have been done in the properties and deformation mechanisms of nanocrystalline materials which are focused on the impact of grain size. Grain size is a dominant effect on dislocation when the size of that is low, but stress besides grain size is another parameter that can be the effect on mechanical structures of nanocrystalline materials. Many of these studies have been done under uniaxial tension or pure shear deformation which in reality they are under mixed loading, and just a few researchers investigate behavior and deformation mechanisms under multi loadings at the atomistic level [20].

The atomic structure and properties of GBs have been an important subject for many years, but the previous work was primarily focused on symmetric GBs with simple structures, and there is limited experiments and simulation worked on the structure and mechanisms of asymmetric GBs. Experimental results show that GBs can significantly affect material properties [21].

Mechanical and thermal properties of materials are dependent on grain boundaries. When the grain size reduced to the nanoscale, there are many features that can be changed and impact on the bulk models. For example, many studies show that when the grain size reaches less than 100 nm, the dislocation activities reduced in the interior of grains [22].

Symmetric and asymmetric tilt GBs for both Cu and Al in the shear response have been studied by Sansoz and Molinari [22], and in their reports, GB-operated deformation mechanisms are related to GB sliding, nucleation of partial dislocations and shear-coupled GB migration which all are GB structure.

Atomic structure of the GB is not unique when the misorientation and inclination of the boundary plane are given. For instance, Cu $\sum 5(310)$ in the MD simulation, the GB change its structure by introducing vacancy effects or changing temperatures [21]. So the simulation models which are only based on the geometrical considerations such

as misorientations and inclination angles are not enough to understand the nature of GB motion. It needs more detail about the effect of GBs on mechanical and kinetic behaviors.

A relaxed GB likes to change structure to the stable state under some conditions like radiation, which may affect the deformation mechanisms and totally mechanical properties of materials.

## 2.4 Grain Size Effect

Grain size is another factor that can be affected by the strength of the material. Reducing this grain size can increase the number of grain boundaries which avoid dislocation motion in the material. Grain sizes over 100 nm the plasticity are dominated by dislocations which came from grain boundary sources. The grain boundary is involved in the whole process when plasticity depends on dislocation motion [14].

Process of Grain boundary relaxation is energy storage, which is released during grain boundary formed defects or disorder as the boundary transform towards an equilibrium configuration. Study of Ni-W showed us hardness would increase hardness up to 35% when the boundary relaxation happened. When the boundaries are relaxed dislocation nucleation, and propagation became difficult and have a better resist grain boundary, and molecular dynamics have confirmed these results.

Chemistry of grain boundary can affect on grain boundary structure, and segregation dopants to nanocrystalline alloys can improve thermal stability, and grain sizes which are controlled by the production of this material and some researchers mentioned that adding dopants can decrease grain boundary energy. Reduction of grain boundaries and the addition of dopants to nanocrystalline material have an influence on the mechanical behavior of the material. Vo et al. confirmed by molecular dynamics simulation that high strength happens by doping in the grain boundaries [15]. Ozerinic, in his experimental tests, confirmed dopants could increase the strength of materials on Cu and Cu-Fe films [16].

## 2.5 Dopant Effects

Mechanical properties of the material give engineers wide ideas to use it in different applications. For example, strengthening mechanisms of materials is one of the properties that separate some materials from others for use in industry. The main factor for causing strength are dislocations. Dislocations have contact with each other by stress, which is available in the materials. Repulsive or attractive interactions can impede dislocation motions some times. in different thermodynamic properties such as temperature and pressure behavior of material will change significantly so grain boundary can behave as a stable interfacial.

One way for strengthening is by adding solute atoms of one element to another, that can see results in the crystal(figure). Yield stress of material increase by solute atoms because they can cause lattice distortions and distortions impede dislocation motion. Solute atoms base on their sizes can act as potential barriers in compressive and tensile stresses to the lattice.

Polycrystalline materials and in this kind of materials, grain size has an essential effect on the mechanical properties because of specific properties of grains such as different orientations that can cause grain boundaries to grow. Grain sizes can effect on yield stress and also by decreasing grain sizes, and yield stress will increase because, in the lattice, we have more free volume.

Strength of material is one of the features of material which is caused the models to be useful in different applications. Construction is evident and primary applicants of this specific property of the material. We have a big building and bridges when we have a durable frame for supporting different tension and compression loadings. For example, steel that is used in the base frame of a building should be strong enough not to bend under weighing of a building or different pressures. Many research needs to be done for increasing strength of materials and expand useful applicant of material in different fields.

Computational simulation is a way for the process of strengthening materials that model material for essential observation elements. When understanding atomistic effects in experimental and information in textbooks about atomistic cannot give us full details, many research turns to molecular dynamic simulation to understand more and get information that is needed. The atomic interaction between atoms can be shown by MD simulation, so dislocation of atoms in the material can be seen in mechanical actions and reaction of atoms. The interatomic potential is used for running simulation to estimate interactions.

These interactions are growing up to millions of atoms for simulating materials more accurately. Molecular dynamics simulation show the results based on equations that are available for increasing strength of the material. This way for getting results is useful in action instead of wasting time and direct observation of experiments.

## 2.6 Deformation Mechanisms

Deformation mechanisms of nanocrystalline metals include GB sliding, grain rotation, diffusional creep, GB migration, dislocation nucleation or absorption at GB.

The atomic structure of GBs has been studied for many years and also much research has been done experimentally by transmission electron microscopy (TEM), and this kind of studies are really hard specifically at high temperatures because low-temperature structure and properties of GBs will be changed by diffusion phenomena and interfacial transitions.

GB motion, which is coupled to shear deformation in both low and high misorientation angle GBs have been studied for many metallic materials. This migration of GBs can be affected in grain growth, nucleation of new grains during recrystallization, and process of material in thermal stability.

Most of the work focus on the sigma 3 because the most common sigma 3 GB is twin boundary with low boundary energy and they, saw it frequently in polycrystals. dislocation nucleation in McDowells investigation for sigma 3 asymmetric boundaries under uniaxial tension showed properties of the material is related to the misorientation between grains and inclination of the GB plane.

Among all deformation mechanisms, shear-stress-induced GB motion, which is GB sliding and GB migration studied more compared with others because it gives deformation mechanisms which are related to exceptional strength and ductility. GB migration is movement of GBs in the perpendicular to the boundary plane, and it is important in atomic rearrangement because it can be effected on recrystallization, grain growth and plasticity of the material. Kaya et al. [23] worked on stress-induced migration for both low-angle and high-angle Al bicrystals at symmetrical (100) GBs and as a result, find out that kinetic properties of GB motion are depended on the misorientation angle.

The disadvantage of experimental investigation is time-consuming while the atomistic simulation is convenience and can be used by high-performance computers and accurate interatomic potentials and especially GB motion is widely used by molecular dynamics because deformation in the simulation is controllable at the atomic scale more detail information can be obtained about deformation mechanisms.

Deformation of metal or alloys produce shear stress which happened by dislocation slip or deformation twinning at low temperatures and low strain rate, but other deformations happened in high temperatures and high strain rates, and it is a common phenomenon that happens in alloys. Stacking faults energy causes twinning in FCC metal. For instance, Wiatom is coarse-grained fcc metal which has high stacking fault energy and deformed by dislocation slip, but Ag atoms have low stacking fault energy and are deformed by twinning.

Two factors can increase the chance of twinning deformation first, high strain rate and second, low deformation temperature. Twinning can happen in perfect or partial dislocations. Interactions between twins and gliding dislocations can be observed by molecular dynamics simulation or in experimental tests.

Twinning effectively can increase the strength and ductility of material simultaneously. In the last decades, invaluable improvement happens for understanding the twinning deformations. One of the features of twinning is mirror symmetry of atomic arrangement at across the grain boundary for FCC metal.

MD simulation has more advantages over experimental studies, which makes it popular and powerful. To add more details, experimental cannot show the atomic level of deformation although MD simulation can show this level by complete details or for deformation behavior like twinning can be investigated in the real-time deformation but this cannot happen experimentally.

Limitation of MD simulation for this part is the small size of models, and many researchers use very small grain size for their models, and this can effect on deformation mechanisms. For example, results that obtained by experimental and MD simulation were not the same for NC Al, Cu, Ni that deformed by twinning. Effect of grain size is so small, and twins are hard to form and time duration is short in MD simulation and as a result strain rate is high while in experimental tests are much higher and comparing these results become complex.

# 3. METHOD

## 3.1 Molecular Dynamics Simulation

Atomic-scale becomes popular these days because it is not easy to see the nanometer scale in the experimental tests, and this method is used to analyze and find out properties of different material in different tests.

The physical movement of atoms and molecules can be investigated by molecular dynamics (MD), which is one of the important computer simulations. This method is used in different fields like biochemistry, nuclear technology, and material science. All the nuclear motion of the constituent particles should follow the classical mechanics in the MD simulation.

Dynamic behavior of material and finding out theoretical methods for the properties of the material in the first-principle calculation because size or number of atoms is limited. Interatomic potential can create millions of atoms in MD simulation, and it is used to find out the mechanical properties of the material and show deformation mechanisms of material.

Result of simulation becomes consistent with experimental results when the computing method is improved, and the atomic level is the basis of all simulations and methods in the material science field. When theoretical methods combined with supercomputers, lots of new information about the behavior of the material in the atomic-level are obtained, which is caused by the birth of computational materials science [37].

Developments in different fields like physics, chemistry, computer science, and graphics can help to have a powerful tool like fast computing systems for material calculations and designs this new technology will help experimental simulations the ability to predict and analyze the properties of the new structure before the creation of the model [38]. Developments of material calculation can improve material science into a scientific quantitative prediction part from the qualitative description of phases [39].

Monte Carlo, Lattice dynamics, and molecular dynamics [40] are a new branch of modern material science which is developed by improving in the material calculation, design, and computer. First person who is used molecular dynamics to study the state equation of gas and liquid in a sphere model was Alder and Wainwright [41] in 1957. They can find out the macroscopic properties of materials by MD simulation. Many research has been done by this method; many improvements need to be done in the future because of some limitations in memory and speed of computers in processing; the simulations are restricted. Great improvements in molecular dynamics happened in the late 1980s with the quick developments of computer technology and multi-body potential function. MD simulations are not so exact in some cases, but the program is simple because of fewer calculations and larger atomic systems.

The interaction between atoms is modeled by the interatomic potential. Therefore, choosing appropriate potential is important and can affect simulation results, and the reliability of simulation is completely related to the reality and accuracy of that potential. Many of these potentials are developed for metallic alloys and mostly used embedded atom method (EAM) in the MD simulation. More information about potentials is available at NIST interatomic potential repository (NIST,IPR) and the knowledge of interatomic models (OPENKIM) which has different potential for various structures.

Stacking fault energy is responsible for the formation of perfect or part of dislocations and ability to cross slip of dislocation and formation of twins. All of these effects that happened by stacking fault energy can effect on strength and hardness of the material. Elastic constants show the response of materials in the elastic deformation stage, which have an influence on yield strength. Therefore, selecting accurate potential to simulate deformation behavior of material and as a result, produce fundamental physical properties of pure model or combination of different elements is important.

### 3.2 Monte Carlo/Molecular Dynamics Simulation

Atomic-scale understanding is important to control the properties of processes in materials. Two main ways usually used, molecular dynamics (MD) and Monte Carlo (MC) simulations. MD simulations are used to show both static and dynamic properties of systems at the atomic level. So, this method is implemented for so many numbers of systems and processes by solving equations of motions to get the trajectory of the particles in phase space for all parts of the system. Therefore, solving the equations will help to yield the positions, velocities of particles, and the forces act on them. Interatomic potential derives forces that should be applied. There are two implications of this simulation. First, this method's result is approximative because of inexact calculated forces. Second, this method is cheap and making calculations with millions of atoms are accessible and also, time that should be spent is longer than the timescale for exact approaches.

MD simulations are limited and needed to be fixed in two parts. First, systems with millions of atoms represent a material on the nanometer to sub-micrometer scale at the solid and liquid state, which is not easy to study [38]. Timescale is the second problem that can be reached, and it makes it difficult when timescales well beyond this limit in the simulation.

The hybrid MC/MD is used for modeling chemical ordering and precipitation in different metal alloys for different heterogeneities like dislocations, grain boundaries, and surfaces. All atoms at the same time displaced in the hybrid MC/MD simulation but in MC only one or two parts are displaced at the same time to obtain high acceptance rate. The displacements in MD simulation are depended on time step because it should be small to conserve the total energy; however, displacements in MC simulation can be large and unphysical.

Duane et al. [37] developed Hybrid MC/MD simulation to combine the advantages of both MD and MC at the same time. This method is time-reversible and uses the symplectic algorithm. The result of hybrid MC simulation is not always better than MD simulation, but sometimes hybrid MC might be better for structures which are not too large.

### 3.3 Crytal Structures

In nature, there are 14 different types of crystal cell structures or lattice, whereas many materials in the world have a unit cell and will be categorized in one of these three types BCC, FCC or HCP. The main difference between all of these models is the structure of the unit cell, for example, BCC structures have some properties, but other structures do not have these features. Some of these features are like the behavior of the material, deformation, density. When working with these materials, understanding these structures are important. Below, we will explain more about these structures.

FCC structures have atoms not only in the corner but also in the center of all cubic faces. Like Bcc structure, the corner atoms are shared among 8 unit cells. In the Fcc structures, the atoms can pack closer together than BCC structures. Packing factor for Fcc structure is 0.74. Aluminum, iridium, copper, gold, lead nickel, platinum, and silver are materials with Fcc structures. This structure is made up of layers of octahedral type planes, and in a sequence of ABCABC and A, B, C are center relative to a closed packed layer.

The number of equidistant nearest neighbors that an atom has is coordination number. For Fcc structure, this number is 12 because the atom in the center of the plane has 6 neighbors in the octahedral plane and 3 neighbors in the below plane. So, total coordination number equals 12. The number for BCC structure is 8 because there is no closed packed atoms and number of neighbors which are close to the center of the unit cell is 8.

Hexagonal close-packed is another common structure unit. The atoms from one layer nest themselves in the empty space between atoms of the adjacent layer just like in the Fcc structure but instead of cubicles hexagon shape is used. This structure has three layers. In the shape of this structure, there are 6 atoms which are arranged in the shape of a hexagon, and the seventh atom is in the middle. The second layer in the middle has three atoms. The coordination number of atoms in the structure is 12.

6 atoms in the close-packed layer. 3 atoms are in the upper layer and 3 in the bottom layer. The packing factor is the same as the FCC structure 0.74. beryllium, cadmium, magnesium, titanium, and zinc are examples of atoms which has HCP structure.

### 3.4 Voronoi tessellation

Tessellation approached on Voronoi diagrams for creating different models and using this is method is increased in the literature about computational mechanics and computer graphics in recent years. Voronoi formalized the n-dimensional case which now we call it Voronoi tessellation  this diagram record information about distances between sets of pints in any dimensional space.

First, William Son used this tessellation for modeling global atmospheric in 1968, which vorticity equations were obtained. Voronoi diagrams can be used in a large number of fields such as science and technology and art. Voronoi tessellation also can be used in practical and theoretical applications like astronomy, epidemiology and computer graphics. Recently they used it also in architecture. Material science used tessellation methods on Voronoi diagrams for modeling structures.

These methods are also useful to obtain various statistics of the corresponding models. They used it because it is a powerful method for modeling and simulating structures with desirable metric and topological properties. There are many ways of constructing Voronoi diagrams. This method that we are using is simple and efficient compared with other methods. First, start with two points on the graph. Voronoi edge is a perpendicular line between two points that are connected to each other. In other cases, if we have three points. The procedures are the same. Calculate perpendicular bisector between each point then remove each section of the perpendicular bisector lines. Now the Voronoi diagram is created.

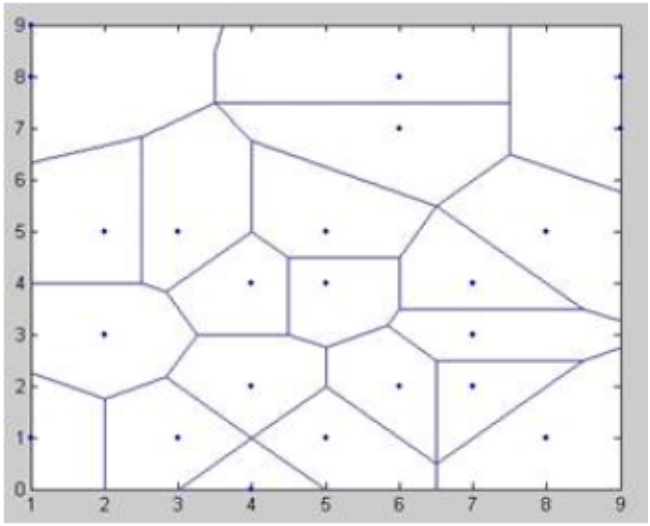

Fig. 3.1. Voronoi Tessellation Model

By increasing the number of points, the number of sites will be increased and also this method can be used for three or more dimensions. Voronoi tessellation is consist of sites or generators that divides the plane. This diagram can be used to solve problems from inside and outside the math world, and it is useful in computational geometry, robotics, and quantization problems.

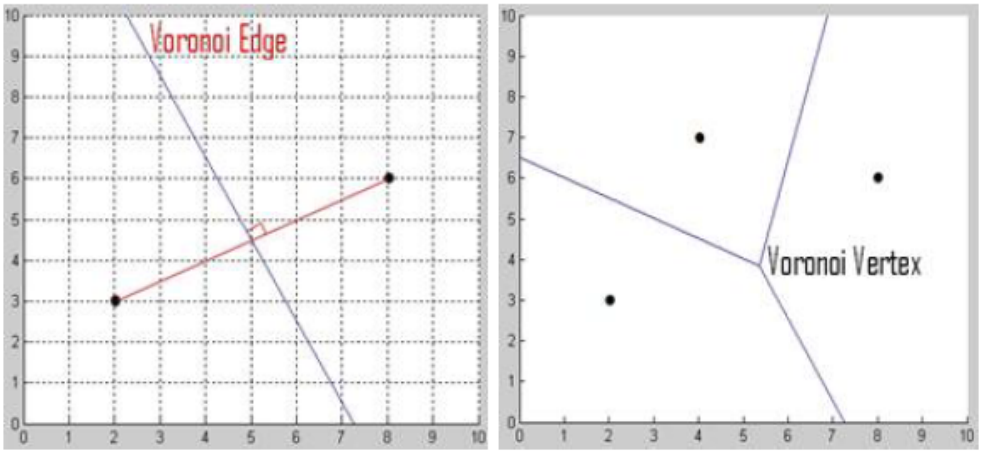


Fig. 3.2. Construction of Voronoi Tessellation

### 3.5 Common Neighbor Analysis

This method is used to analyze structure that is more complex, high dimensional signatures to see obviously arrangements of atoms to better understanding different structures. This method is one of the popular methods for analysis. In this method, the characteristic signature is computed from the topology of bonds that neighbor atoms are connected to that. Usually, we call two atoms are neighbor when they are within specified cutoff distance r of each other. A number of neighbor atoms are an important parameter in the analysis method, which is mentioned by Tsuzuki et al [29]. chemical species of common neighbors is added when the CNA extended to binary atomic systems.

The common neighbor analysis is introduced by honey-cut and Anderson. the CNA shows the structural ordering around pairs of a particle in terms of shared neighboring particles. The CNA is an algorithm which is used to characterize the local structural crystalline systems. The goal of this analyze is to understand precisely the phase of atoms and defects that are associated with these atoms.

There are three different modes for common neighbor analysis:

1. Conventional CNA:

   In this mode, for defining the pair of atoms is bonded or not, we should determine cutoff distance. This is selected based on crystal structures. For Fcc and Hcp structure this radius must lie between the first and second shell of neighbors but for Bcc is between second and third neighbor shell. There is a list of optimal cutoff distances for FCC and Bcc structures.

2. Adaptive CNA:

   This method is used when it is difficult to choose the right cutoff radius for the conventional CNA, specifically in multiphase systems, and that is a reason adaptive CNA is developed. This method is proposed by Stokowski et al. to determine the optimal cutoff for individual particles [30].

3. Bond-based CNA:

   Based on the existing network of bonds between the particles, the CNA indices are computed. The bonds should be defined in this method. The modifier outputs the computed per bond as a new bond property for using in further statistical analyses. The modifier, according to the structure, categorized each particle. The structural types are defined as integer numbers.

   - 0 = Other, unknown coordination structure
   - 1 = FCC, face-centered cubic
   - 2 = HCP, hexagonal close-packed
   - 3 = BCC, body-centered cubic
   - 4 = ICO, icosahedral coordination

A complete set of input particles are needed to perform the analysis for CN modifier.

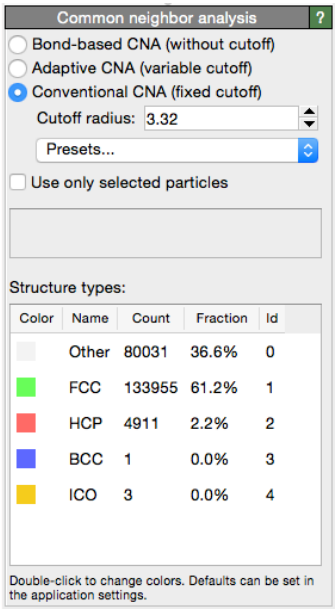


Fig. 3.3. Common Neighbor Analysis

Ovito is an open scientific visualization tool which analyzes atomistic and particle simulation data to obtain better what is happening in material and physical properties. This software has an open source license, and it is a powerful tool to analyze, understand, and illustrate simulation results.

Modeling material with the atomic-scale resolution is MD,Ms static, and MC simulation. The output of this simulation is atomistic configuration or trajectories, which needs to analyze to produce new scientific views. Powerful analysis and visualization are important factors in analyze, and without that, key information will remain unknown, undiscovered, inaccessible, and unused.

Ovito is a software to help scientist translate the raw atomic positions into a meaningful graphical picture. Ovito is written in C++ that can be used in all major operating system. For availability of this software for researchers and scientists, it has been released under terms of GNV public license.

Therefore, Ovito can be used free, and everyone can contribute to the software, extend, or newly developed. This software is developed by Dr. Alexander Stokowski at the material department of Missouri state university.the first version of this software was published in December 2009. nowadays, more than 10000 used it in different fields such as computational physics, material science, and chemistry. We want to explain the common analysis of this software in the following.

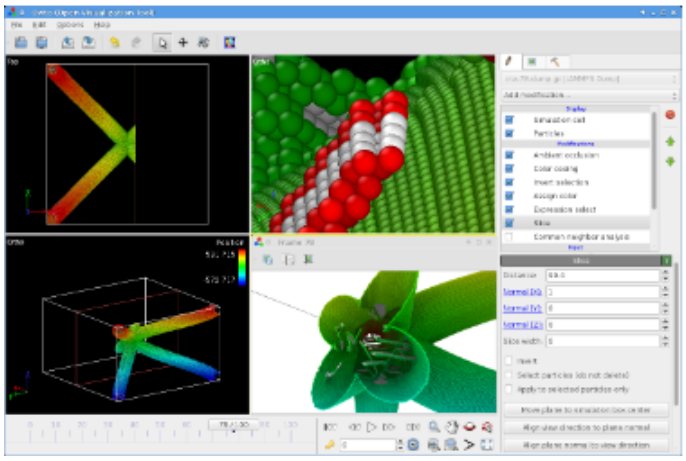

Fig. 3.4. Ovito Software

# 4. SIMULATION OF POLYCRYSTALLINE ALUMINUM

## 4.1 Computational Details

Voronoi tessellation procedure is used here to create nanocrystalline Al. Voronoi is a popular way that can make a different structure for different materials. We explain this tessellation in the method part. Challenging part for this section is selecting appropriate dimensions for simulation cube. The dimensions of the simulation cube were selected to be 200 Å, 200 Å, and 200 Å along the x, y, and z directions, respectively.

In this simulation box, we placed 12-grain centers randomly. In this part, the crystal orientation for each grain was randomly assigned to model the average behavior of bulk polycrystalline samples effectively. Each grain according to its crystal orientation are filled by Al atoms

After the creation of the model, the 3D polycrystal model contained 483,197 atoms, and the average grain size by using a spherical grain assumption was estimated to be about 10 nm. Boundary conditions Periodic boundary conditions were applied in all directions. In order to avoid unphysical interaction between neighboring atoms, atoms that are closer than 0.2 Å from another atom were removed from the model.

A Finnis-Sinclair (F-S) type of interatomic potential [31] was used to describe the Al-Al, Mg-Mg, and Al-Mg interactions due to the better reproducibility of thermal and mechanical properties of Al-Mg alloys. The bulk phase diagram of Al-Mg was better reproduced by this potential than other available Al-Mg potentials [32, 33]. Specifically, the solidus and liquidus lines are correctly reproduced by this F-S potential at the Al-rich side of the phase diagram [31] and the composition of Al-5at.%Mg for this work is within in this range.

To create NC Al-Mg models with an equilibrium distribution of Mg atoms, we employed hybrid Monte Carlo/molecular dynamics (MC/MD) simulations to introduce Mg atoms into the NC Al model, rather than directly placing the Mg atoms at the GBs or the grain interior [34]. Hybrid MC/MD [35,36] has been a useful tool to help to achieve an equilibrium distribution of dopants in matrix atoms. In hybrid MC/MD simulations, the atomic structural relaxations are realized by MD running, and the MC scheme samples the semi-grand canonical ensemble. MC swaps of Al atoms with Mg atoms are performed, and the swap probability is dictated by the Metropolis criterion in specified temperatures. All atoms move according to the regular MD time integration, and the time step is 0.1 fs. The hybrid MC/MD simulation is considered to reach equilibrium if the fluctuation of total energy over the last 10,000 steps is less than 0.5%. A chemical potential difference of 1.9 eV between Mg and Al was used in the hybrid MC/MD simulation to achieve 5 at.% Mg in our model. The 5 at.% of Mg dopants was chosen in this study because Al-Mg alloys with an Mg content in the range of 1-5 at.% have been widely used in practical engineering applications. The model was relaxed to achieve both mechanical and chemical equilibrium while keeping the system temperature at 300K and the pressure equal to zero. During the uni-axial tensile simulation, straining was carried out along the x-direction, while the other two directions were free to expand or shrink. A constant strain rate was applied to both NC Al and Al-Mg alloys. A small time step of 0.1 fs was used for time integration in solving the equation of motion during the simulations. The tensile simulations were carried out using the NPT ensemble with the temperature of 300K and zero pressure. All simulations were performed using the LAMMPS [37]. The software of OVITO [38] was used for the visualization of the atomic structures.

## 4.2 Results

In this paper, we create a fully relaxed NC Al 5at% Mg model that is shown in Fig 4.1. We select different colors for different atoms. These colors are selected base on

common neighbor analysis (CNA) Values. FCC structures like Al atoms are colored in green, but Al atoms that are available in grain boundaries are colored in blue. We select the red color for Mg dopants to view the distribution of Mg in the model obviously as we mentioned in the introduction, our goal for this thesis is explaining the effect of Mg dopants in the Nanocrystalline Al.

Mg distribution can be visible more by cutting the model in different slices. So, in order to visualize the distribution of atoms a cross-section of 3D model is shown in Fig 4.1b. in this figure density of Mg, atoms are selected to be large to see clearly the distribution of atoms in this slice. Slices in the model show Mg atoms are distributed more in the grain boundaries, but it is available in another part of grains. Next step

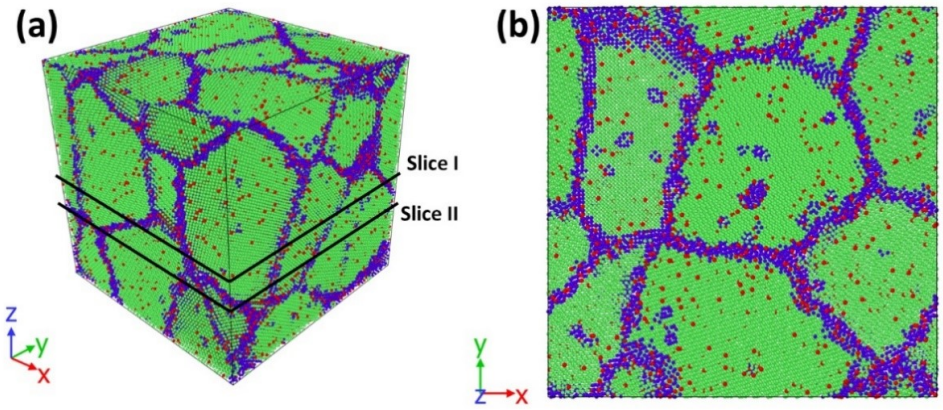


Fig. 4.1. A fully relaxed nanocrystalline Al-5at.%Mg alloy (a) 3D model and (b) Slice II: a cross-section parallel to the x-y plane. The Al atoms with fcc structure are colored green; the Al atoms at GBs are colored blue, and the red atoms with a larger size are Mg atoms.

after the creation of both models, Al and Al-Mg alloys, is applying tension loading at temperature 300 k. these loadings are applying in two different strain rates. Strain rate 9 and 10 are chosen for this simulation to see and compare the effect of strain rate on the results.

Fig 4.2 is shown stress-strain curves for all four samples in one graph. The color of curves for pure Al models are black and for Al-Mg alloys are red. In this graph, solid lines are selected for strain rate 9, while dash lines are chosen for strain rate 10. As

the graph shows, Mg atoms can affect the strength of Nanocrystalline Al. ultimate stress, the highest amount of stress is for Al-Mg 5% for strain rate 9. Strength stress consisted of yield strength and ultimate strength, which stress-strain curves for Al-Mg samples have higher value compare with Pure material. As it was mentioned in the previous part, pun et al. s result have the same result in an experimental test with our result in this simulation which Mg atoms can improve the strength of a material when it is added to Nanocrystalline Al [2].

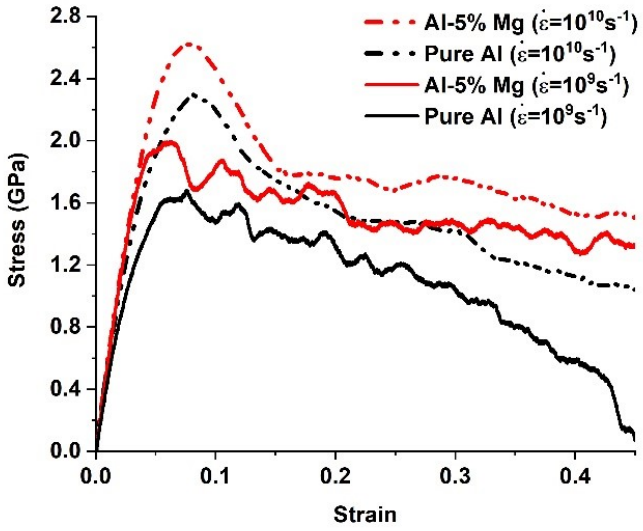


Fig. 4.2. Stress-strain curves obtained from tensile simulations of nanocrystalline pure Al and Al-5%Mg alloy at two different strain rates

Two different strain rate are selected for Al-Mg alloys to see the effect of Mg on pure Al. strain rate 10 has a larger strength for both Al and Al-Mg alloys. Mg dopants can increase the ultimate stress in both strain rates. Ultimate stress for pure Al is almost 1.8 Gpa for strain rate 9 whereas adding Mg dopants to Al can increase this strength up to 2 GPa. The similar finding can be obtained for strain rate 10. Ultimate stress will increase from 2.2 in a pure model to .5 Gpa by adding 5at% Mg to nanocrystalline Al.

The strain is selected to be up to 0.4, and as it is showing the graphs for all samples, ultimate stress happens before strain 0.15, and the behavior of materials changes a lot after this point. For example, pure Al in strain rate 9 will drop quickly and failing happens in the structure, but for the al-mg model in this strain rate, it did not happen at all.

When we compare two different strain rate for single Al-Mg model, we can say that stress is higher in strain rate 10 in different strains, so flow stress for strain rate 10 is larger than strain rate 9. The same result happens for pure Al, and strain rate 10 has larger stress compare with strain rate 9.

As stress-strain shows, the effect of Mg on Nanocrystalline Al is obvious. Simulation from here and Lee and pun from experimental results confirmed that Al-Mg alloys have better ductility and strength in compare with Pure Al. Here we can explain more about the effect of Mg dopants, two slices of our model were cut from Al and Al-Mg 3D model alloys that are from strain rate 9. These slices in these strains are selected to show the effect of dopants and behavior of materials when tension loading applied to the model.

Tensile loading is applied in the Y direction for our models so, slices should be cut in XY plane and Z direction. Two slices in two different positions of z-direction are chosen for explaining more. Slice 1 is showing the position of $z = -4$ for both materials. The thickness for this slice is 6 to view the structure of atoms obviously. Figure 4.3 shows this slice in different strains for both Al and Al-Mg samples. The top figure is for pure nanocrystalline Al in strains up to 0.2, and bottom pictures are for Al-Mg in the same strains.

Colors for the atoms are selected based on common neighbor analysis (CAN) values. The Al atoms have different colors in different structural properties of the material in the model. FCC structures are green and HCP structures are brown and blue color is selected for disordered structures. Larger atoms with red colors are Mg atoms that are distributed in the models. Stacking faults with hcp structure have brown colors in different figures in Al-Mg. amorphous regions are colored in blue.

Pure model when the strain increase after reaching the ultimate point, stress quickly drops, and by viewing that slice in that time we can see in figure C, fracture starts to grow. In the following figures, this fracture increases in strain 0.2, and as a result slope of stress-strain curve became negative and dropping so quickly.

Position of slice 2 is $Z = -40$ that is shown in figure 4.4 and same as figure 4.3 in XY plane but applied strain is up to 0.4, and thickness for this slice is 10. Same colors are used for this slice. We labeled three different grains for tracking the behavior of models in different strains during tensile loadings. In this slice, fracture happens later compare with slice $z = 13$. Strain 0.3 is the start point for both model that crack starts in this slice, and it can continue as it is shown in figure D and H.

Fig 4.5a shows deformation twinning that happens in Al-Mg 5% in fig 4.4 that is applied strain of 0.2 in slice 2. Figure 4.5b is a close view of showing twinning in the structure

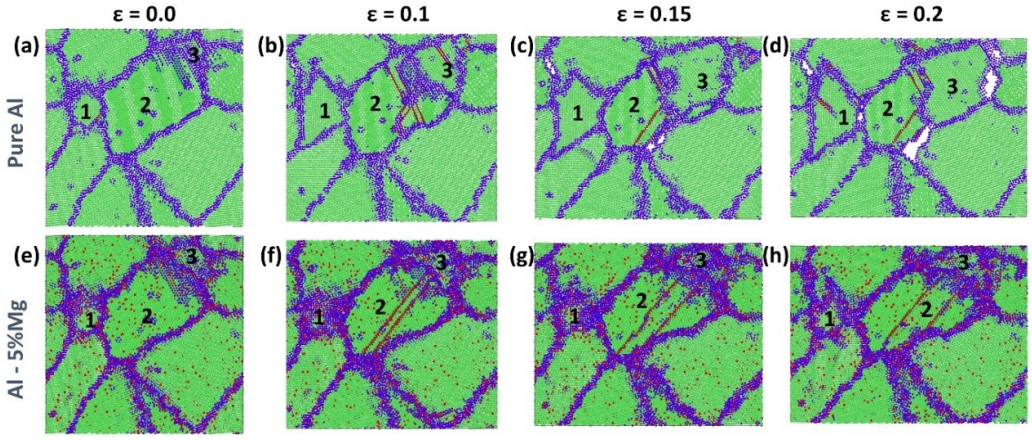


Fig. 4.3. Atomic structure for Slice I of the nanocrystalline pure Al and Al-5at.%Mg alloy models at different applied strains

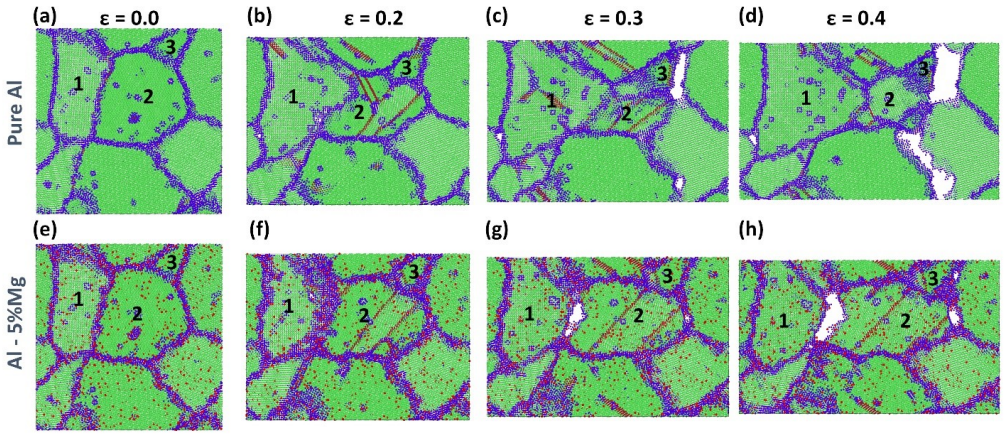


Fig. 4.4. Atomic structure for Slice II of the nanocrystalline pure Al and Al-5at.%Mg alloy models at different applied strains.

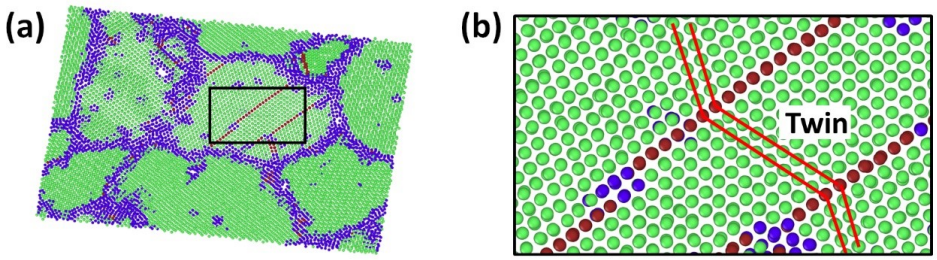


Fig. 4.5. Atomic structure of the observed deformation twinning in Al-5at.%Mg alloy at the applied strain of 0.2: (a) Slice II in Fig. 4.4(f) which are rotated to clearly show the twinning, (b) a close-up view of the deformation twin.

## 4.3 Discussion

In order to identify the mechanisms for improving the strength of NC Al through doping Mg atoms, we monitored the motions and size changes of grains during the tensile simulations. Different GB induced deformation mechanisms were identified, including dislocation nucleation from GB and deformation twinning in both pure Al and Al-Mg alloy. For example, Fig.4.5 shows the atomic structure of the deformation twin observed in Al-5at%Mg alloy at the applied strain of 0.2. The results of pure Al

show that the GB migration was frequently observed in pure Al in order to accommodate the deformation during the tensile loading. However, it was difficult to find GB migrations in the Al-Mg alloys. As shown in Fig. 4.3(a)-(d) for pure Al, the sizes of Grain #1 and #3 increased with the increasing strain, while the size of Grain #2 decreased. The comparison of the sizes of these three grains clearly shows that the size ratio between grains changed during the tensile loading due to the migrations of GBs between the neighboring grains. However, for the same slice in the Al-Mg alloy model shown in Fig. 4.3(e) to (h), the change in the size ratio between Grains #1, #2, and #3 are very small and negligible.

Similar findings can be obtained from analyzing the results of a different slice shown in Fig. 4.4. The size ratio between Grain #1 and Grain #2 changed for pure Al by Fig. 4.4 (a)-(d) while the change in the size ratio is much smaller for the Al-Mg alloy as shown in Fig.4.4(e)-(h). This dopant pinning effect on GB migration agrees well with a study by Rahman et al. [39]. A simple tilt GB model was used in their study, and artificial driving force (ADF) techniques were used to induce GB motions. They found that a strong dopant pinning effect was observed at different misorientations. In this study, we used fully 3D nanocrystalline models to reveal the Mg dopant pinning effects on GB migration in NC Al. All these results clearly indicate that the addition of Mg atoms can effectively impede the GB migration in NC Al, and hence improve its strength at the early deformation stage up to a strain of 0.2.

The analysis of the failure process of pure Al and Al-Mg indicates that Mg atoms can also effectively prohibit the nucleation of intergranular cracks in NC Al. The ultimate failure of both NC pure Al and Al-Mg alloy were caused by the initiation of intergranular cracks from the regions close to triple junctions and their propagation along the GBs in the materials. This failure mechanism agrees well with the finding from a study by Hocker et al. [40]. They observed inter-granular fracture in both pure Al and Al-Mg alloy but didnt find any difference in tensile strength between them. However, in our study, we found that the strength of the Al-Mg alloy is higher than

pure Al. The strengthening mechanism includes the effect of dopants on prohibiting crack initiation in Al-Mg alloys. As shown in Fig. 4.3 (c) for pure Al at the applied strain of 0.15, cracks nucleated at triple junctions near Grain #1 and #2 in pure Al. However, no cracks were observed for Al-Mg alloys at the strain of 0.15 and even up to 0.2, as shown in Fig. 4.3(g) and (h). The addition of Mg dopants leads to the formation of a larger disorder GB region and triple junction region compared to the pure Al model, as shown the comparison between Fig. 4.3(b) and 4.3(f). The larger disorded triple junction region can better accommodate the deformation triple junctions and hence prohibit the initiation of crack from triple junctions, as shown in Fig. 4.3 (c) and Fig. 4.3 (g).

Moreover, Mg atoms segregated to GBs can affect the flow stress of NC Al through impeding the propagation of existing intergranular cracks. As shown in Fig. 4.4 (c) and (d), the crack near Grain #3 is propagating quickly in pure Al when the applied strain increases from 0.3 to 0.4. Compared to pure Al, the propagation of the crack between Grain #1 and #2 in Al-Mg alloys is much slower with the strain increased from 0.3 to 0.4, as shown in Fig. 4.4(g) and (h). The larger amorphous GB regions induced by segregation of Mg atoms act as stronger barriers to the propagating cracks in the Al-Mg alloy. All these results suggest that Mg dopants segregated to GBs can strengthen the NC Al through effectively prohibiting the nucleation of intergranular cracks and impeding the propagation of existing cracks.

The stability of nanocrystalline materials can be improved by GB doping to suppress the driving force for grain coarsening. For example, the experiments of sputter-deposited Al alloy [18] show that the grain size of Al-Mg alloys was found to be much smaller than that of pure Al, though they were treated at the same conditions. Doping with different elements have been widely used to stabilize the grain size of nanocrystalline materials against the increase of temperature.

In this study, we illus-trate that Mg dopants can effectively stabilize the grain size during the deformation process of NC Al due to the pinning effect of dopants on GB migrations. This result indicates that GB doping could be an effective strategy for controlling the grain size of nanocrystalline materials during manufacturing processes that utilize deformations, such as severe plastic deformation (SPD) techniques.

# 5. BICRYSTAL ALUMINUM

## 5.1 Computational Details

Simulations in this part are similar to previous part. The MD code LAMMPS is used with the modified embedded-atom method potential for Al while MC simulation used the parallel MC algorithms developed by Sadigh et al. [35]. The latter alternates MC switches of atomic species (swaps) with MD runs which are used in LAMMPS. When we put two different oriented crystal lattices together at a planar interface parallel to one of the surfaces, the bicrystal model is created. In this part, we have different bicrystal models in this part. $\sum 5$ and $\sum 3$ are two bicrystal model that we are particulary interested in. For creating one of this model, for example, $\sum 5$, the bottom grain rotates about the [001] tilt axis by $\theta/2$ in a clockwise direction and the top grain in the anticlockwise direction. The GB plane was the (110) for $\sum 3$ and (211) for $\sum 5$ crystallographic plane of the bottom grain and the plane of (1 -10) and (2-10) for bottom grain.

The dimensions of the simulation box were selected to be 10 10 and 10 along the x, y and z directions, respectively. After the creation of this model, the 3D bicrystal model contained 124,416 atoms. Boundary conditions were applied periodically in the three directions; therefore, during system relaxation isobaric-isothermal (NPT) is used in all three dimensions. In this study, the simulation temperature was set to 300K. before applying shear loading, it needs to remove some atoms that are close to each other which here we tried to delete atoms that interact each other and delete atoms that are closer than 0.2 to avoid unphysical interaction between neighboring atoms.

There are many potentials that can be used for Al materials in the molecular dynamics simulation, we choose the newest potential which is published in 2018 by

Dickel [41] because it can be useful for very large c/a ratio and allow the atomistic modeling of a wide class of alloys containing material properties for the pure state and MEAM potential foe Mg-Al-Zn system which allow modeling wide range of alloys which contains Mg atoms. This potential can produce Al-Mg alloys, which contain 5 wt% Mg is within this range.

The bulk phase of Al-Mg was produced by this potential, which is new, and there is not that much available research that used this potential before. This potential cannot be used for a model that has an hcp ground state and c/a ratio greater than ideal.

Both GBs consist of topologically identical structural units; their differences are only in the distance which separates structural units and positions from the GB plane. Bicrystal Al-Mg models for both models with an equilibrium distribution of Mg atoms are made by using hybrid Monte Carlo/molecular dynamic (MC/MD) simulation which here we introduce Mg atoms randomly instead of choosing an exact position in pure Al model at the grain boundaries. Zhang et al. [42] also studied about $\sum 5$ (310) GB structures in bicrystal Al and structure of GB on its mechanical and kinetic properties under shear stress at low temperature ($T = 10K$) with different deformation mechanisms and GB migration were also observed.

MD part is running to relax the atomistic structure, and MC scheme sampled the semi-grand canonical ensemble. This simulation let the model determine the relaxed concentration and atom distribution in the model for selected chemical potential differences of the constituents. Structural relaxation and thermal vibrations are also employed besides the exchange of atom types.

Time step is 0.1 fs, and all atoms change their positions in the MD time integration, and figures show the distribution of Mg atoms in Al alloys in both models, and it needs total energys fluctuation over last 10000 steps should be less than 0.5%.

The potential chemical difference in this model which change the number of segregated atoms in the model is 2.1 eV between Mg and Al elements and used in the

hybrid MC/MD simulation to achieve 3.5 at.% Mg. we choose this percentage because potential recommend this range 1-8 wt% Mg should be distributed in Al models.

The applied strain rate for both models is $10^9$, which is fixed in the process of the running simulation. Equation of motion is solved during the small time step of 0.1 fs during this simulation. NPT ensemble during shear loading is implemented for 300k temperature and zero pressure. LAMMPS and OVITO are used for running MD simulation and and analyzing results

## 5.2 Results

A fully relaxed bicrystal Al model is shown in Fig. 5.1 in which the atoms are colored based on their common neighbor analysis (CNA) values. The green color is for FCC structures of Al atoms. Red colors are HCP colors which are distributed in grain boundary plane. We have two bicrystal models which cross- section of these models, $\sum 3$ and $\sum 5$ are shown in Fig. 5.2. Figures of 5.2b and 5.2d clearly show the distribution of Mg atoms in both upper and bottom grain boundaries. Blue color shows Mg atoms in both models, and this observation showed Mg atoms also could be distributed in the grain boundary plane. White color are atoms which are not categorized as FCC or Hcp structures. As the figures showed, Mg atoms are distributed randomly in the grain. Figure 5.2a shows the structure of the grain boundary plane in $\sum$ 3 and degree of between two grains is presented in the figure. Figure 5.2b represents this structure in $\sum$ 5 with a different angle between grains. Brown and purple color show this structure in $\sum$ 3 and $\sum$ 5.

After creating the model and distribution of Mg in both models, we should apply shear loading at temperature 300 k. The strain rate for all the models are fixed at 109. Here, Fig. 5.3 showed stress-strain curve for $\sum$ 5 and $\sum$ 3 for pure Al. The orange line is for Al in $\sum$ 5 structure, and blue color is selected to be the Al model in $\sum$ 3 structure. As it is shown in Fig. 5.3, $\sum$ 3 has higher strength and ultimate stress compared with $\sum$ 5.

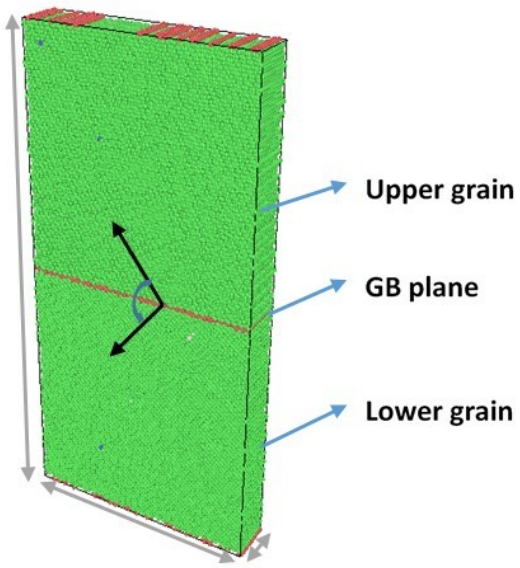


Fig. 5.1. A Fully Relaxed $\sum$ 3 Bicrystal Model

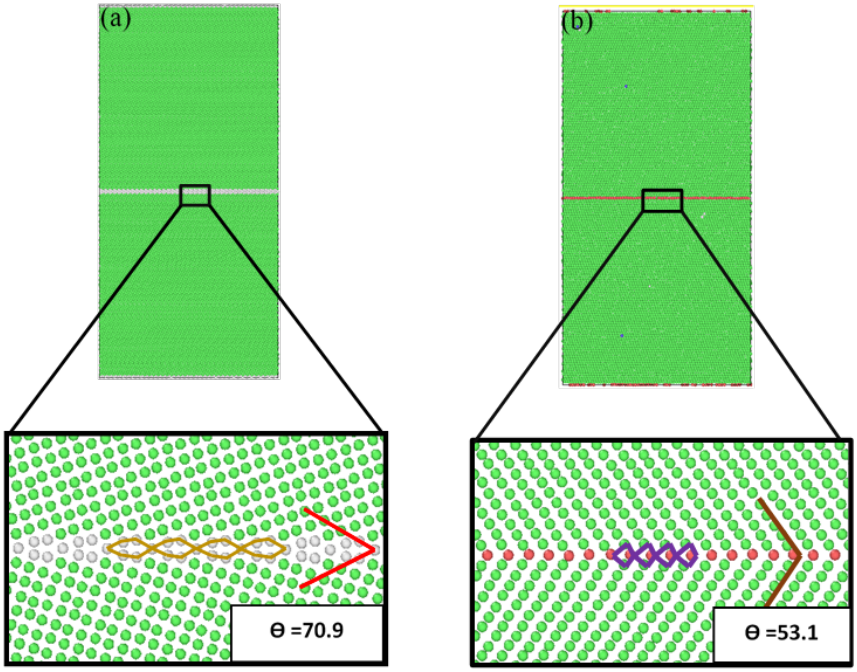


Fig. 5.2. structure of atoms in (a) $\sum$ 5 (b) $\sum$ 3

Here, we compared different pure models that are created and applied shear stress to see the behavior of materials in Fig. 5.4. We select a different color for different models. Here the strain rate is also constant. The strain for this graph is up to 0.25, and observation of this graph showed the behavior of $\sum 3$ is completely different from other structures.

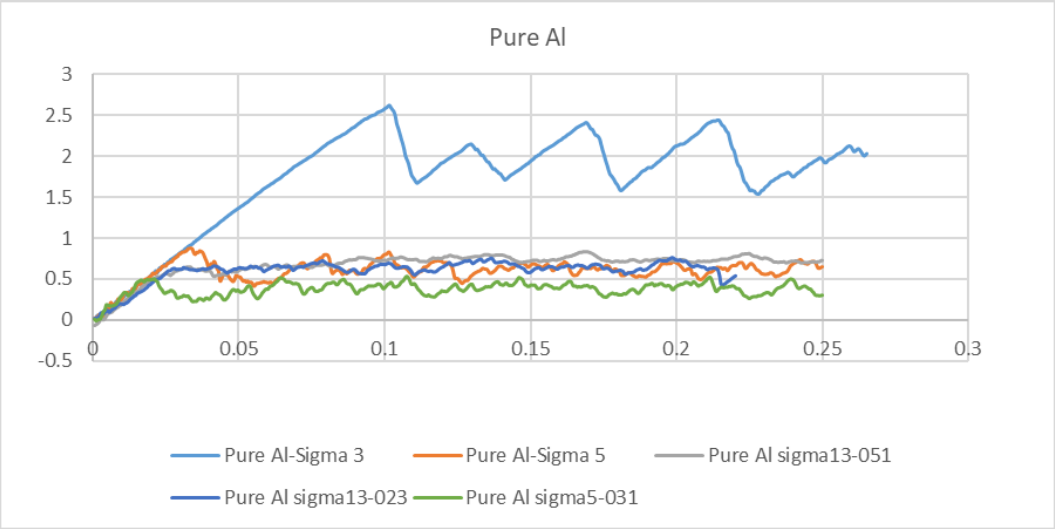


Fig. 5.3. Stress-Strain Curve Obtained from Shear Stress of Pure Al Models

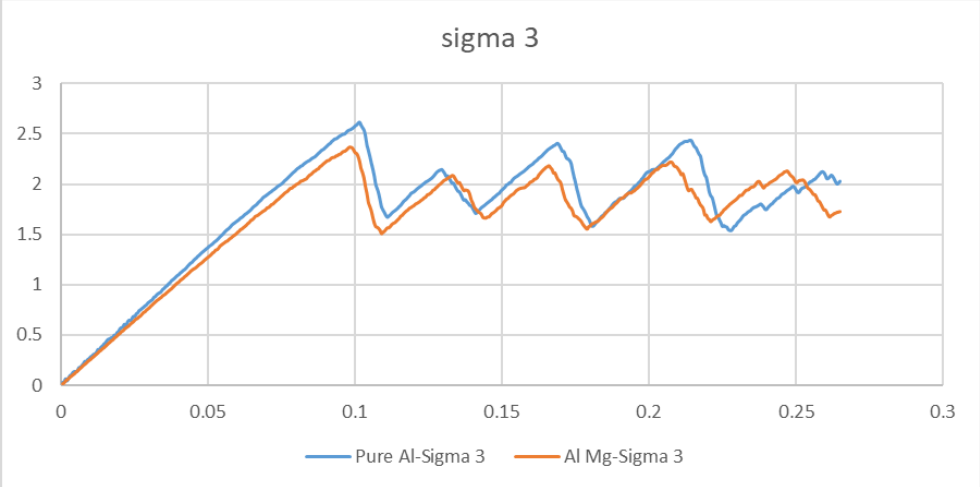


Fig. 5.4. Stress-strain curve obtained from Shear loading of Al And Al-Mg $\sum 3$ models

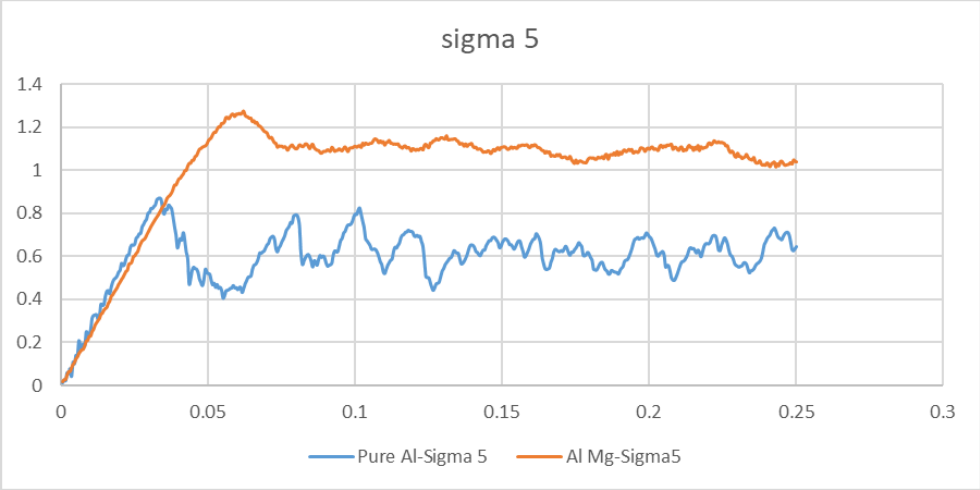


Fig. 5.5. Stress-strain curve obtained from Shear loading of Al And Al-Mg $\sum$ 5 models

In this part, we showed figures that the effect of dopants on the nanocrystalline model is shown. Figure 5.4 is for $\sum$ 3 model, and Fig. 5.5 shows $\sum$ 5 for both Al and Al-Mg models. As it is shown in the figures, Mg dopants can increase strength and ultimate stress in different strains in $\sum$ 5 model, but this effect is not obvious in $\sum$ 3. The blue color is selected to be a pure Al model, and orange is shown Al-Mg model.

We compare the effect of dopants in different models. Besides $\sum$ 3 and $\sum$ 5, we also created other GBs, such as $\sum$ 13, $\sum$ 9, $\sum$ 27 and $\sum$ 29. All of them are applied shear loading and strain is up to 0.25. Different colors are selected for different models. As shown in Fig. 5.6, the behavior of some of these models are the same, but $\sum$ 3 has different behavior by adding this amount of Mg to Al.

Figure 5.7 below shows the movement of atoms in the $\sum$ 3 model when the strain increases and as it shows, selected atoms can pass grain boundary plane, which is showing the effect of shear loading in moving atoms. Also, this happens for the $\sum$ 5 model. This figures showed selected atoms before reaching grain boundary, on the grain boundary and when these atoms passed grain boundary in applied shear loadings.

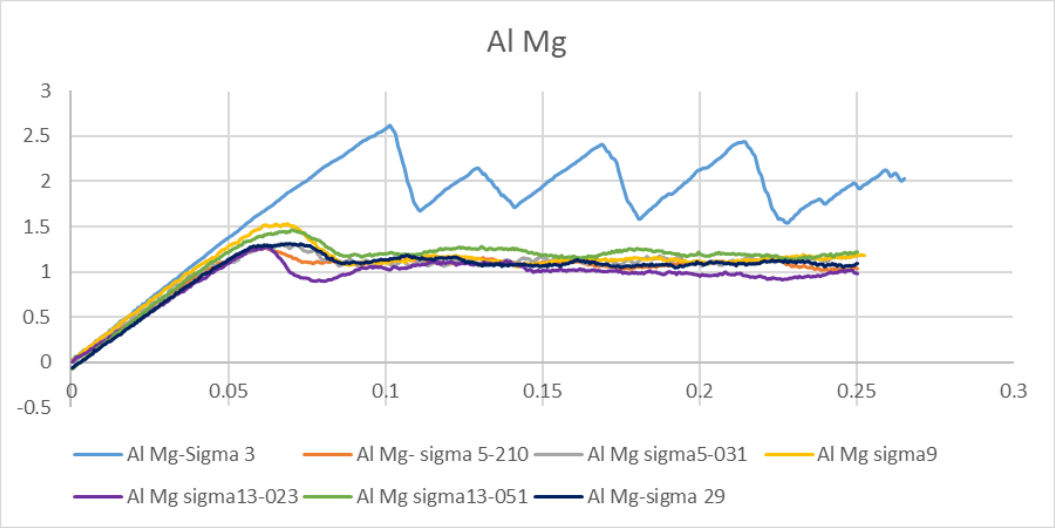


Fig. 5.6. Stress-strain curve obtained from shear stress of Al-Mg Alloys

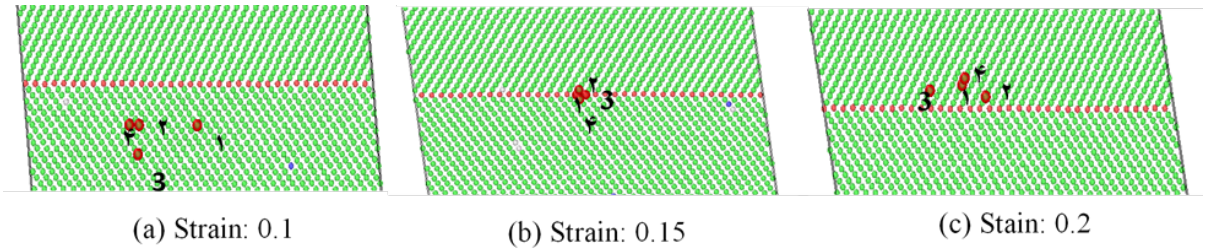


Fig. 5.7. Migration of atoms in $\sum$ 3 bicrystal model

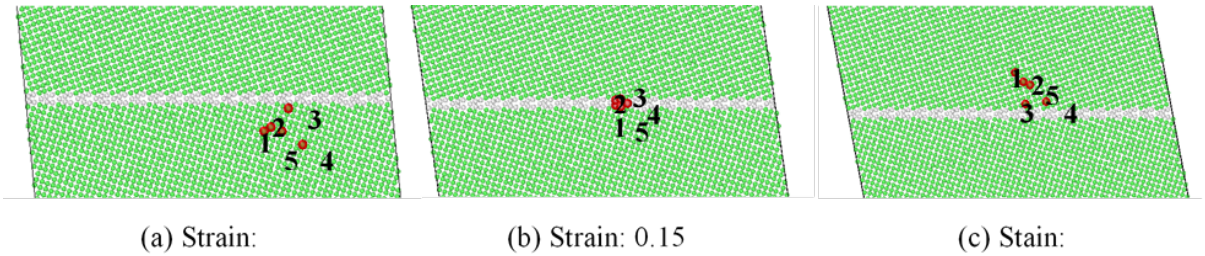


Fig. 5.8. Migration of atoms in $\sum$ 5 bicrystal model

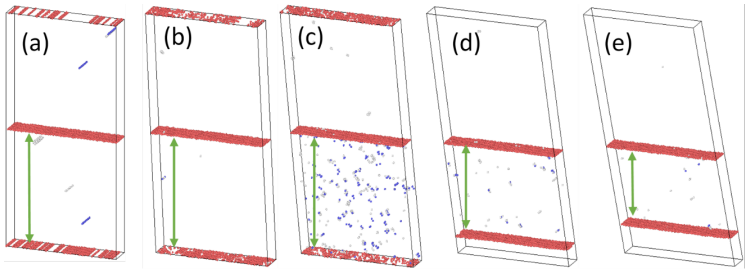


Fig. 5.9. Atomic structure of Al $\sum$ 3 at different applied strains (a)0 (b)0.05 (c)0.1 (d)0.15 (e)0.2

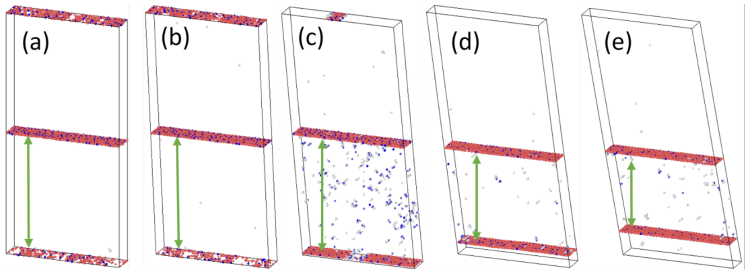


Fig. 5.10. Atomic structure of Al-Mg $\sum$ 3 at different applied strains (a)0 (b)0.05 (c)0.1 (d)0.15 (e)0.2

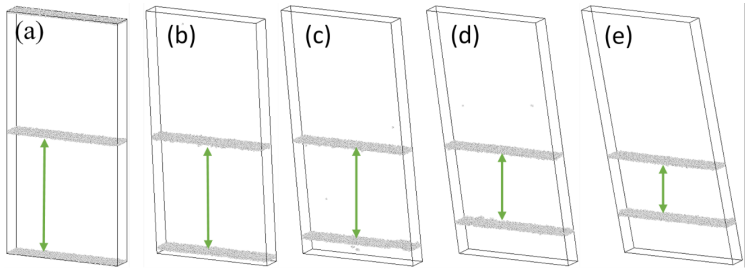


Fig. 5.11. Atomic structure of Al $\sum$ 5 at different applied strains (a)0 (b)0.05 (c)0.1 (d)0.15 (e)0.2

Following figures wants to show Gb migration in different strains, which is for both $\sum$ 3 and $\sum$ 5 both pure Al and Al-Mg samples. These figures clearly show the effect of Mg dopants in these model and speed of migration when the shear loading applied in all models.

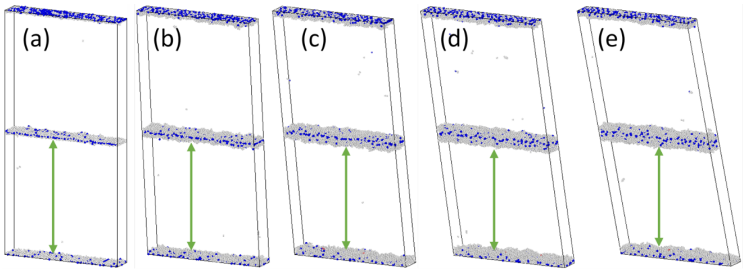


Fig. 5.12. Atomic structure of Al-Mg $\sum$ 5 at different applied strains (a)0 (b)0.05 (c)0.1 (d)0.15 (e)0.2

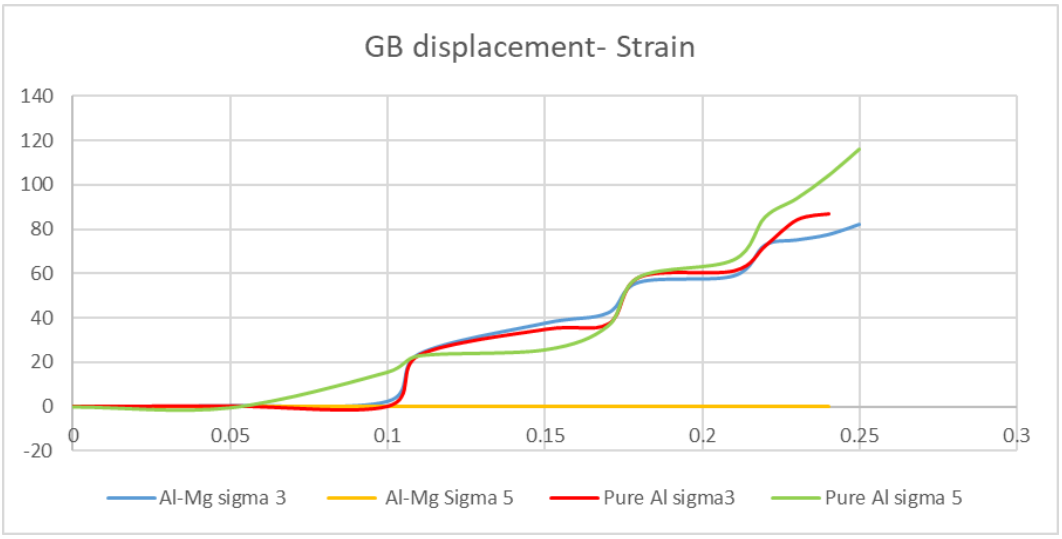


Fig. 5.13. Grain boundary displacement-Strain curve for bicrystal models

## 5.3 Discussion

To understand the behavior of material for the effect of dopants in the strength of pure Al models, we applied shear loading for all samples. Results of Fig.13 shows that before the addition of dopants to the material, because of the structure of the model and compact distribution of atoms, the ∑3 model has higher strength compared with other models. Flow stress is another point that can be observed in the stress-strain curves, and as it showed, the flow stress of ∑ 3 model is much greater than ∑ 5 model.

To show the effect of the grain boundary plane in different bicrystal models, we examined different structures and understand the behavior of other models is similar to the behavior of ∑ 5. The arrangement of atoms at GBs is different from the ∑ 3 model because the atoms are so close to each other in this model, which can help improve stress in applied loading. As a result in the stress-strain curve, we can see the fluctuation of ∑ 3 model because of the small size and closeness of atoms is more than others, which is normal in this case.

Similar findings can be obtained by adding dopants. We precisely see the stress-strain curves in Fig. 16 and it showed that Mg dopants could improve the strength of the material in another model, but this change in stress cannot reach to ultimate stress in the ∑ 3 models with blue color in the figure. This graph also can confirm previous findings, which showed the behavior of other structures is not different from ∑ the 5 models in shear loading tests.

If we compare both pure models and Al-Mg models for same material like ∑ 3, it can be visible that Mg dopants not only cannot effect on the strength of material but also in some strains have less amount of stress compared with Al model but influence of Mg dopants on ∑ 5 models showed it could improve stress significantly and huge fluctuation of the pure model removed when dopant added. Thus the structure of atoms and the position of big size dopants like Mg in the nanocrystalline Al can help changes in the behavior of the material in different tests.

GB migration is shown to see the effect of shear loading on different strains. For pure models, it showed at the early deformation, grain boundaries are stable in their positions, but at the last steps, these grain boundaries will become closer in the strain up to 0.2 for ∑3 bicrystal model. When the Mg dopants added to NC Al, this happens again for ∑3, and the figures are not different from the pure model.

In ∑5 model, the graph showed GB migration is faster than ∑3 which is shown deformation happened in the early stage of this material and when the dopants added to material the place of the grain boundary fixed and by increasing strain there is no movement in this plane, and just thickness of GB planes will increase which is caused improving strength of material compared with the pure model.

To explain more, we focus on the motion of GB in all samples, and the effect of adding dopants was realized by GB migration. The snapshots in figures 19-22 showed that Mg atoms could change the motion of GB. When Mg atoms added to ∑ 5 pure models, the thickness of GB will be increased although shear responses of the ∑ 5 pure model are completely different and distance between GBs decreases the when strain increases up to 0.2. Based on structure and angle of atoms, when Mg dopants added to the pure model, the number of atoms in GB will increase. So, by increasing the number of atoms in GB, the thickness of GB will increase, and the stress of the material will improve; however, it did not happen in sigma 3 models.

Fig.19 which is shown GB motion in different strains for pure model sigma 3 acts like sigma 5 model and GB planes become closer when shear loading applied to the models, but when we add dopants to sigma 3 models, changes in thickness and number of Mg dopants in GB are not more than another model.

When we observe the Fig.19 GB plane start to move in Fig 19 (c) and velocity of GB plane increase rapidly in the following fig.19 (d) and (e). Also, at the same time GB movement happened for Al-Mg model in fig. 20. it will start to be close to another plane after strain 0.1. when we compare both pure model in different strains, we can find out GB plane movement in sigma 5 model start earlier than sigma 3 model. by comparing the last two models in strain 0.2, GB planes in sigma 3 models are closer than sigma5 model because of the different structure and behavior of models in applied shear stress.

The behavior of GB plane in Al-Mg sigma 5 model is not similar to sigma 3 model because instead of moving planes in this structure, distribution of Mg atoms increase in the grain boundaries and did not let the GB plane to move. it is caused changing the behavior of the material in two different structures when dopants added to the pure model.

Fig 23 confirms our results for GB migration in all samples. When we calculate the distance between GB planes, Mg dopants cannot change the behavior of pure Al in sigma 3 model, blue and red lines which are pure Al and Al-Mg model has similar GB displacements in different strains, but in sigma 5 model there is no displacement in Al-Mg model. pure model this graph confirmed that velocity of GB displacement is more than another sigma 3 models

Movement of dopant atoms in different structures can be seen in figures 20 and 22. When dopants added to the pure model in Fig.20, we can find out those atoms in the GB plane are more mobile than the pure model. It can be concluded that Mg atoms tended to be distributed in another part of the structure instead of the GB plane. However, for Al-Mg model in Fig.22, when the thickness of GB increased, a number of atoms in GB will be increased, which showed number of Mg atoms go up in strain up to 0.2.

We concluded that GB migration was sensitive to GB structure and behavior of bicrystal models in shear loading for selected structures are entirely different, and dopants in some cases based on properties of the material can be caused to have better structure.

# 6. CONCLUSIONS AND FUTURE WORKS

## 6.1 Conclusions

The strength of NC Al can be improved by doping 5at% Mg from atomistic simulation results. Grain boundary migration can accommodate the deformation when the tensile loading is applied to nanocrystalline Al. Simulation results show that Mg dopants can help to stop GB migration in NC Al, which lead to the improved strength of the material at the early deformation stage. Furthermore, another dopant effect is that the dopants segregated to GBs can effectively prohibit nucleation of intergranular cracks, and also stop the propagation of existing intergranular cracks along GBs. This effect can help the improvement of flow stress for Al-Mg compared with pure Al. Controlling the grain size is the promising application of dopants, which improves stability of nanocrystalline materials during deformation processes.

The results of bicrystal models show that grain boundaries character could affect the strength of materials. The results indicate that the $\sum 3$ GB, which is a twin boundary, has higher strength and flow stress than $\sum 5$ and other GBs. The results also show that adding Mg dopants cam improve the strength and flow stress of $\sum 5$ and other GBs. Howver, this influence is not observed in the $\sum 3$ GB. Analysis of atomic structures shows that adding Mg dopants stops GB migration in $\sum 5$ and other GBs. However, it cannot impede GB migration in the $\sum 3$ GB.

## 6.2 Future Works

The effect of Mg dopants on the NC Al is studied in our study. However, it still needs more work to be done for dopant effect on NC Al. Some of the issues and challenges of the current study that needs further research are listed below:

- We applied tensile loading for both polycrystalline materials, but compression loading can be tested in the future and investigate the effect of dopants in the compression loadings
- This study has been done for the effect of first dopants in the models but the effect of second dopants can be studied in the future time especially the effect of Zn dopants in the Al-Mg alloys
- In the bicrystal model part of our research, we can try to run the simulation for tensile and compile loadings for both models and also the effect of second dopants on the nanocrystalline Al can be investigated.

# REFERENCES

# REFERENCES


[1] I. Ovid'Ko, R. Valiev, and Y. Zhu, "Review on superior strength and enhanced ductility of metallic nanomaterials," *Progress in Materials Science*, vol. 94, pp. 462–540, 2018.

[2] S. C. Pun, W. Wang, A. Khalajhedayati, J. D. Schuler, J. R. Trelewicz, and T. J. Rupert, "Nanocrystalline al-mg with extreme strength due to grain boundary doping," *Materials Science and Engineering: A*, vol. 696, pp. 400–406, 2017.

[3] T. Chookajorn, H. A. Murdoch, and C. A. Schuh, "Design of stable nanocrystalline alloys," *Science*, vol. 337, no. 6097, pp. 951–954, 2012.

[4] M. Rajagopalan, M. Bhatia, M. Tschopp, D. Srolovitz, and K. Solanki, "Atomic-scale analysis of liquid-gallium embrittlement of aluminum grain boundaries," *Acta Materialia*, vol. 73, pp. 312–325, 2014.

[5] J. Luo, "Stabilization of nanoscale quasi-liquid interfacial films in inorganic materials: a review and critical assessment," *Critical reviews in solid state and materials sciences*, vol. 32, no. 1-2, pp. 67–109, 2007.

[6] J. Luo , "Interfacial engineering of solid electrolytes," *Journal of Materiomics*, vol. 1, no. 1, pp. 22–32, 2015.

[7] B.-H. Lee, S.-H. Kim, J.-H. Park, H.-W. Kim, and J.-C. Lee, "Role of mg in simultaneously improving the strength and ductility of al–mg alloys," *Materials Science and Engineering: A*, vol. 657, pp. 115–122, 2016.

[8] D. L. Olmsted, L. G. Hector Jr, and W. Curtin, "Molecular dynamics study of solute strengthening in al/mg alloys," *Journal of the Mechanics and Physics of Solids*, vol. 54, no. 8, pp. 1763–1788, 2006.

[9] P. R. Cantwell, M. Tang, S. J. Dillon, J. Luo, G. S. Rohrer, and M. P. Harmer, "Grain boundary complexions," *Acta Materialia*, vol. 62, pp. 1–48, 2014.

[10] T. Frolov and Y. Mishin, "Phases, phase equilibria, and phase rules in low-dimensional systems," *The Journal of chemical physics*, vol. 143, no. 4, p. 044706, 2015.

[11] W. D. Kaplan, D. Chatain, P. Wynblatt, and W. C. Carter, "A review of wetting versus adsorption, complexions, and related phenomena: the rosetta stone of wetting," *Journal of Materials Science*, vol. 48, no. 17, pp. 5681–5717, 2013.

[12] T. Hu, S. Yang, N. Zhou, Y. Zhang, and J. Luo, "Role of disordered bipolar complexions on the sulfur embrittlement of nickel general grain boundaries," *Nature communications*, vol. 9, no. 1, p. 2764, 2018.

[13] S. Yang, N. Zhou, H. Zheng, S. P. Ong, and J. Luo, "First-order interfacial transformations with a critical point: breaking the symmetry at a symmetric tilt grain boundary," *Physical review letters*, vol. 120, no. 8, p. 085702, 2018.

[14] T. Frolov, M. Asta, and Y. Mishin, "Phase transformations at interfaces: observations from atomistic modeling," *Current Opinion in Solid State and Materials Science*, vol. 20, no. 5, pp. 308–315, 2016.

[15] T. Frolov, M. Asta, and Y. Mishin , "Segregation-induced phase transformations in grain boundaries," *Physical Review B*, vol. 92, no. 2, p. 020103, 2015.

[16] Y. Mishin, W. Boettinger, J. Warren, and G. McFadden, "Thermodynamics of grain boundary premelting in alloys. i. phase-field modeling," *Acta Materialia*, vol. 57, no. 13, pp. 3771–3785, 2009.

[17] T. Frolov, S. Divinski, M Asta, and Y. Mishin, "Effect of interface phase transformations on diffusion and segregation in high-angle grain boundaries," *Physical review letters*, vol. 110, no. 25, p. 255502, 2013.

[18] A. Devaraj, W. Wang, R. Vemuri, L. Kovarik, X. Jiang, M. Bowden, J. R. Trelewicz, S. Mathaudhu, and A. Rohatgi, "Grain boundary segregation and intermetallic precipitation in coarsening resistant nanocrystalline aluminum alloys," *Acta Materialia*, vol. 165, pp. 698–708, 2019.

[19] X. Sauvage, N. Enikeev, R. Valiev, Y. Nasedkina, and M. Murashkin, "Atomic-scale analysis of the segregation and precipitation mechanisms in a severely deformed al–mg alloy," *Acta Materialia*, vol. 72, pp. 125–136, 2014.

[20] D. Zhao, O M Løvvik, K. Marthinsen, and Y. Li, "Segregation of mg, cu and their effects on the strength of al $\sigma$5 (210)[001] symmetrical tilt grain boundary," *Acta Materialia*, vol. 145, pp. 235–246, 2018.

[21] L. Zhang, Y. Shibuta, C. Lu, and X. Huang, "Interaction between nano-voids and migrating grain boundary by molecular dynamics simulation," *Acta Materialia*, vol. 173, pp. 206–224, 2019.

[22] L. Zhang, C. Lu, and Y. Shibuta, "Shear response of grain boundaries with metastable structures by molecular dynamics simulations," *Modelling and Simulation in Materials Science and Engineering*, vol. 26, no. 3, p. 035008, 2018.

[23] G. Sainath and B. Choudhary, "Molecular dynamics simulation of twin boundary effect on deformation of cu nanopillars," *Physics Letters A*, vol. 379, no. 34-35, pp. 1902–1905, 2015.

[24] B. R. Brooks, R. E. Bruccoleri, B. D. Olafson, D. J. States, S. a. Swaminathan, and M. Karplus, "Charmm: a program for macromolecular energy, minimization, and dynamics calculations," *Journal of computational chemistry*, vol. 4, no. 2, pp. 187–217, 1983.

[25] C. L. Brooks III, "Simulations of protein folding and unfolding," *Current opinion in structural biology*, vol. 8, no. 2, pp. 222–226, 1998.

[26] A. Chakrabartty and R. L. Baldwin, "Stability of $\alpha$-helices," in *Advances in protein chemistry*. Elsevier, 1995, vol. 46, pp. 141–176.

[27] W. D. Cornell, P. Cieplak, C. I. Bayly, I. R. Gould, K. M. Merz, D. M. Ferguson, D. C. Spellmeyer, T. Fox, J. W. Caldwell, and P. A. Kollman, "A second generation force field for the simulation of proteins, nucleic acids, and organic molecules," *Journal of the American Chemical Society*, vol. 117, no. 19, pp. 5179–5197, 1995.

[28] Y. Duan and P. A. Kollman, "Pathways to a protein folding intermediate observed in a 1-microsecond simulation in aqueous solution," *Science*, vol. 282, no. 5389, pp. 740–744, 1998.

[29] H. Tsuzuki, P. S. Branicio, and J. P. Rino, "Structural characterization of deformed crystals by analysis of common atomic neighborhood," *Computer physics communications*, vol. 177, no. 6, pp. 518–523, 2007.

[30] A. Stukowski, "Structure identification methods for atomistic simulations of crystalline materials," *Modelling and Simulation in Materials Science and Engineering*, vol. 20, no. 4, p. 045021, 2012.

[31] M. Mendelev, M. Asta, M. Rahman, and J. Hoyt, "Development of interatomic potentials appropriate for simulation of solid–liquid interface properties in al–mg alloys," *Philosophical Magazine*, vol. 89, no. 34-36, pp. 3269–3285, 2009.

[32] B. Jelinek, J. Houze, S. Kim, M. Horstemeyer, M. Baskes, and S.-G. Kim, "Modified embedded-atom method interatomic potentials for the mg- al alloy system," *Physical Review B*, vol. 75, no. 5, p. 054106, 2007.

[33] X.-Y. Liu, P. Ohotnicky, J. Adams, C. L. Rohrer, and R. Hyland Jr, "Anisotropic surface segregation in al mg alloys," *Surface science*, vol. 373, no. 2-3, pp. 357–370, 1997.

[34] R. I. Babicheva, S. V. Dmitriev, L. Bai, Y. Zhang, S. W. Kok, G. Kang, and K. Zhou, "Effect of grain boundary segregation on the deformation mechanisms and mechanical properties of nanocrystalline binary aluminum alloys," *Computational Materials Science*, vol. 117, pp. 445–454, 2016.

[35] B. Sadigh, P. Erhart, A. Stukowski, A. Caro, E. Martinez, and L. Zepeda-Ruiz, "Scalable parallel monte carlo algorithm for atomistic simulations of precipitation in alloys," *Physical Review B*, vol. 85, no. 18, p. 184203, 2012.

[36] J. Schäfer, A. Stukowski, and K. Albe, "Plastic deformation of nanocrystalline pd–au alloys: on the interplay of grain boundary solute segregation, fault energies and grain size," *Acta Materialia*, vol. 59, no. 8, pp. 2957–2968, 2011.

[37] S. Plimpton, "Fast parallel algorithms for short-range molecular dynamics," *Journal of computational physics*, vol. 117, no. 1, pp. 1–19, 1995.

[38] A. Stukowski, "Visualization and analysis of atomistic simulation data with ovito–the open visualization tool," *Modelling and Simulation in Materials Science and Engineering*, vol. 18, no. 1, p. 015012, 2009.

[39] M. J. Rahman, H. S. Zurob, and J. J. Hoyt, "Molecular dynamics study of solute pinning effects on grain boundary migration in the aluminum magnesium alloy system," *Metallurgical and Materials Transactions A*, vol. 47, no. 4, pp. 1889–1897, 2016.

[40] S. Hocker, M. Hummel, P. Binkele, H. Lipp, and S. Schmauder, "Molecular dynamics simulations of tensile tests of ni-, cu-, mg-and ti-alloyed aluminium nanopolycrystals," *Computational Materials Science*, vol. 116, pp. 32–43, 2016.

[41] D. E. Dickel, M. I. Baskes, I. Aslam, and C. D. Barrett, "New interatomic potential for mg–al–zn alloys with specific application to dilute mg-based alloys," *Modelling and Simulation in Materials Science and Engineering*, vol. 26, no. 4, p. 045010, 2018.

[42] L. Zhang, Y. Shibuta, X. Huang, C. Lu, and M. Liu, "Grain boundary induced deformation mechanisms in nanocrystalline al by molecular dynamics simulation: From interatomic potential perspective," *Computational Materials Science*, vol. 156, pp. 421–433, 2019.